Plant community shifts as early indicators of abrupt permafrost thaw and associated carbon release in an interior Alaskan peatland.

William Dale Cox[1], Catherine Dieleman[2], Thomas A Douglas[3], Evan S Kane[4], Rebecca B Neumann[5], Eugenie Susanne Euskirchen[6], and Merritt R Turetsky[1]

[1]University of Colorado Boulder
[2]University of Guelph
[3]CRREL Alaska
[4]Michigan Tech University
[5]University of Washington
[6]University of Alaska Fairbanks

November 27, 2024

Abstract

Widespread changes to near-surface permafrost in northern ecosystems are occurring through top-down thaw of near-surface permafrost and more abrupt localized thermokarst. Both types of thaw are associated with a loss of ecosystem services, including soil hydrothermal and mechanical stability and long-term carbon storage. Here, we analyze relationships between ground layer vegetation, active layer thickness, and greenhouse gas fluxes along a thaw gradient from permafrost peat plateau to thaw bog in Interior Alaska. We used active layer thickness to define four distinct stages of thaw: Stable, Early, Intermediate, and Advanced, and we identified key plant taxa that serve as reliable indicators of each stage. Advanced thaw, with a thicker active layer and thermokarst, was associated with increased abundance of graminoids and Sphagnum mosses but decreased plant species richness and ericoid abundance. Early thaw, driven by active layer thickening with little visible evidence of thermokarst, coincided with a fivefold increase in CH4 emissions, accounting for ˜30% of the total increase in methane emissions occurring in ˜10% of the timeline of the forest-to-bog transition. Our findings suggest that early stages of thaw, prior to the formation of thermokarst features, are associated with distinct vegetation and soil moisture changes that lead to abrupt increases in methane emissions, which then are perpetuated through ground collapse and collapse scar bog formation. Current modeling of permafrost peatlands will underestimate carbon emissions from thawing permafrost unless these linkages between plant community, nonlinear active layer dynamics, and carbon fluxes of emerging thaw features are integrated into modeling frameworks.

Hosted file

`WCOX_early_thaw_JGR_Biogeosciences.docx` available at https://authorea.com/users/852160/articles/1243886-plant-community-shifts-as-early-indicators-of-abrupt-permafrost-thaw-and-associated-carbon-release-in-an-interior-alaskan-peatland

Plant community shifts as early indicators of abrupt permafrost thaw and associated carbon release in an interior Alaskan peatland.

W. D. Cox[1,2], C. M. Dieleman[3], T. A. Douglas[4], E. S. Kane[5,6], R. B. Neumann[7], E. S. Euskirchen[8], and M. R. Turetsky[1,2]

[1]Department of Ecology and Evolutionary Biology, University of Colorado Boulder, Boulder, Colorado, USA.

[2]Renewable and Sustainable Energy Institute, University of Colorado Boulder, Boulder, Colorado, USA.

[3]School of Environmental Science, University of Guelph, Guelph, Ontario, Canada.

[4]US Army Corps of Engineers Cold Regions Research and Engineering Laboratory, Fort Wainwright, Alaska, USA.

[5]College of Forest Resources and Environmental Science, Michigan Technological University, Houghton, Michigan, USA.

[6]USDA Forest Service, Northern Research Station, Houghton, Michigan, USA.

[7]Department of Civil and Environmental Engineering, University of Washington, Seattle, Washington, USA.

[8]Institute of Arctic Biology, University of Alaska Fairbanks, Fairbanks, Alaska, USA.

Corresponding author: William Dale Cox (william.cox-2@colorado.edu)

Key Points:

- Emerging thaw features can be identified by predictable species turnover in the plant community.
- Methane emissions increase five-fold during early onset of boreal peatland permafrost thaw.
- Net ecosystem CO_2 exchange is more resilient than methane emissions to the effects of early thaw.

Abstract

Widespread changes to near-surface permafrost in northern ecosystems are occurring through top-down thaw of near-surface permafrost and more abrupt localized thermokarst. Both types of thaw are associated with a loss of ecosystem services, including soil hydrothermal and mechanical stability and long-term carbon storage. Here, we analyze relationships between ground layer vegetation, active layer thickness, and greenhouse gas fluxes along a thaw gradient from permafrost peat plateau to thaw bog in Interior Alaska. We used active layer thickness to define four distinct stages of thaw: Stable, Early, Intermediate, and Advanced, and we identified key plant taxa that serve as reliable indicators of each stage. Advanced thaw, with a thicker active layer and thermokarst, was associated with increased abundance of graminoids and Sphagnum mosses but decreased plant species richness and ericoid abundance. Early thaw, driven by active layer thickening with little visible evidence of thermokarst, coincided with a fivefold increase in CH_4 emissions, accounting for ~30% of the total increase in methane emissions occurring in ~10% of the timeline of the forest-to-bog transition. Our findings suggest that early stages of thaw, prior to the formation of thermokarst features, are associated with distinct vegetation and soil moisture changes that lead to abrupt increases in methane emissions, which then are perpetuated through ground collapse and collapse scar bog formation. Current modeling of permafrost peatlands will underestimate carbon emissions from thawing permafrost unless these linkages between plant community, nonlinear active layer dynamics, and carbon fluxes of emerging thaw features are integrated into modeling frameworks.

1 Introduction

Permafrost stores approximately 1,000 ± 150 Pg of carbon in the upper 3 m of soil, corresponding to ~60% of the Earth's terrestrial soil carbon pool (Hugelius *et al*., 2014). Including carbon pools residing in deeper soils, permafrost currently stores more than twice the amount of carbon (C) in the atmosphere (Hugelius *et al*., 2014; Hugelius *et al*., 2020). These carbon stores have amassed over thousands of years as cold climates that form and maintain permafrost severely limit microbial activity and organic matter decomposition. However, polar amplification of ongoing climatic warming and an increase in frequency of extreme weather events are destabilizing permafrost globally (Schuur *et al*., 2015; Biskaborn *et al*., 2019). The combination of increased surface temperatures and increased rainfall has been identified as a major driver of thaw, as well as thaw-driven methane emissions, at northern latitudes (Neumann *et al*., 2019; Douglas *et al*., 2020; Mekonnen *et al*., 2021). During gradual permafrost thaw, a thickening of the seasonally thawed active layer affects centimeters of surface permafrost over years to decades (Douglas *et al*., 2021). Permafrost can also thaw abruptly, affecting meters of the soil profile over months to years through land subsidence and thermokarst. Thermokarst most commonly occurs in ice-rich permafrost settings. However, since ground ice content can vary widely, it is difficult to predict where, when, and at what rates thermokarst will occur (Osterkamp *et al*., 2009). Both gradual and abrupt thaw lead to vegetation changes and the release of stored permafrost carbon as CO_2 and CH_4 to the atmosphere (Schuur *et al*., 2015). Due to differences in permafrost carbon release between gradual vs. abrupt thaw scenarios (Turetsky *et al*., 2020) as well as uncertainties in potential

vegetative biomass, it is unclear whether permafrost ecosystems will become a globally significant source of carbon to the atmosphere or whether these systems will remain a net carbon sink under projected climate change (McGuire *et al*., 2018, Turetsky *et al*., 2020).

Approximately half of northern peatlands are underlain by surface permafrost (Hugelius *et al*., 2020). Chronosequence studies across peatlands varying in time-since-thaw in western Alaska, USA reported that up to 30% of the permafrost peat carbon pool is lost in the first few decades following thaw (Jones *et al*., 2017; O'Donnell *et al*., 2012). On the other hand, a chronosequence study in northern Alberta, Canada, found minimal evidence of intensified decomposition following thaw and instead found that permafrost carbon loss post-thaw was more than offset by modern carbon accrual via biomass and peat accumulation (Heffernan *et al*., 2020). The discrepancy between these studies is likely due to different types or ages of permafrost peat that will affect the bioavailability of carbon to microbial processing during and after thaw (Manies *et al*., 2021; Dieleman *et al*., 2016; Dieleman *et al*., 2022). Post-thaw carbon balance also depends on the cycling of other nutrients that can become more bioavailable for plant or microbial activity (Salmon *et al*., 2018), which in turn can stimulate plant productivity and associated carbon accrual (Schuur *et al*., 2008; Salmon *et al*., 2016; McGuire *et al*., 2018; Albano *et al*., 2021). To date, our understanding of abrupt thaw impacts on carbon storage or emissions in permafrost peatlands is based on studies that compare permafrost peatlands to thermokarst collapse bogs that have undergone at least several decades of thaw. These studies quantify the net change in carbon pools between distinct ecosystem states, but they do not explore changes that occur during state transitions (here, from surface permafrost to an established collapse bog state following thermokarst). Thus, there has been little opportunity to examine the potential changes in permafrost carbon release in the initial stages of permafrost thaw, despite many laboratory-based soil incubation studies indicating significant amounts of carbon mineralization occurring immediately upon thaw (Schädel *et al*., 2016). Based on these incubation studies, it is likely that current global methane emission models are underestimating contributions from early thaw.

Vegetation community structure in permafrost systems represents a potential tool for identifying emerging abrupt thaw events. As ice-rich permafrost decays, local environmental conditions are affected that alter hydrologic conditions, soil temperature, soil nutrient availability, and microbial processes. Macrofossil and pollen analyses have demonstrated that in northern permafrost regions these shifting abiotic conditions could result in conversion of forest ecosystems dominated by terrestrial species into an aquatic thermokarst wetland community (Beilman & Robinson, 2003; Yang *et al*., 2010; Jones *et al*., 2013). However, there has been little documentation of plant species turnover during the transition from stable permafrost to early thaw states. Because moss species distributions tend to be strongly governed by local environmental conditions (e.g., Stewart & Mallik, 2006; Frego, 2007; Hylander, 2009; Patiño & Vanderpoorten, 2018), it seems likely that the peatland moss community may serve as a reliable and useful indicator of ecosystem state and integrity during the early stages of permafrost thaw.

Here our goal was to investigate active layer thickness (ALT) as a measure of surface permafrost change and its relationships with a changing plant community composition and carbon fluxes along a spatial gradient from an intact permafrost peat plateau into a thermokarst collapse bog in Interior Alaska. Along this spatial gradient, our dataset also captured a time series in which our plots experienced top-down thaw of near-surface permafrost over the course of our three-year sampling period.

We expected the ground layer moss community to respond quickly to the changes in local microclimate and soil substrate structure triggered by permafrost thaw, allowing us to explore whether there were any species-level changes that could be used as a predictor of the early onset of permafrost thaw. We hypothesized that: (1) thaw of ice-rich permafrost peat was associated with increases in soil C fluxes to the atmosphere during active layer thickening before thermokarst initiation due to subtle changes in microtopography that had influenced soil moisture, and (2) because ground-layer plant communities were sensitive to changes in microclimate, plant community change in response to active layer thickening would allow us to identify plant species usable as an early indicator of permafrost change.

2 Materials and Methods

2.1 Site description

Our study site is part of the Alaska Peatland Experiment (APEX) within the Bonanza Creek Long Term Ecological Research site (BNZ LTER) located in the Tanana River Valley, approximately 30 km southwest of Fairbanks, Alaska, USA. The climate is continental subarctic with long cold winters and a comparatively short summer growing season. Annual temperatures range from -50 ℃ in winter to 30℃ in the summer, with a mean annual total snowfall of 1.7 m (Jorgenson *et al*., 2001), which represents 40%–45% of annual precipitation (Liston and Hiemstra, 2011). The site is within the discontinuous permafrost region but is located entirely on peat plateaus underlain by near-surface permafrost. Peat plateaus are permafrost peatlands composed of gravel, silt, and sand at depth overlain by 1-5 m of organic matter and vegetation. In this location the plateaus rise above fens and other wetland features that are typically not underlain by near-surface permafrost (Jones *et al*., 2013; Jorgenson *et al*., 2020). The upper few meters of permafrost can be considered syngenetic, while deeper layers are epigenetic (Jones *et al*., 2013). Permafrost in the Fairbanks area has undergone multiple aggradation and degradation phases, with the most recent maximum permafrost extent coinciding with the “Little Ice Age” in the 14th century CE (Jones *et al*., 2013; Jorgenson *et al*., 2020). Within the Tanana River Valley, permafrost thickness can reach up to 47 m, although it’s only a few meters at the APEX peatland complex (Chacho *et al*., 1995; Jones *et al*., 2013). Though fire is an important factor in both permafrost thaw and community succession in the boreal biome, we lack a detailed fire history of the site. However, there is no evidence of fire in the peat plateau in the last 50 years. The study site encompasses the features of an actively expanding thermokarst collapse bog and surrounding forested permafrost peat plateau within the greater peatland complex (Figures 1a and 1b). Radiocarbon dating suggests the center of our thermokarst collapse bog formed approximately 380 years before the present (Jones *et al*.,

2013; Klapstein *et al*., 2014). Active subsidence continues to occur at the margins and recent studies show that the rates of lateral thaw degradation have been increasing in the past two decades (Neumann *et al*., 2019; Euskirchen *et al*., 2024).

Vegetation in the study area is typical of interior Alaska lowlands. The area is sparsely treed, and most of those trees are black spruce (*Picea mariana* (Mill.) Britton, Sterns & Poggenb.). American larch (*Larix laricina* (Du Roi) K. Koch) is also present, primarily in open bog areas. The understory consists mostly of shrubs (*Betula glandulosa* Michx., *Salix* spp.) and ericoids (*Rhododendron tomentosum* Harmaja, *Vaccinium* spp., *Chamaedaphne calyculata* (L.) Moench, etc.). The ground layer ranges from feather mosses (*Hylocomium splendens* (Hedw.) Schimp., *Pleurozium schreberi* (Willd. ex Brid.) Mitt., and others) and the drier end of the *Sphagnum* spectrum (*Sphagnum fuscum* (Schimp.) H. Klinggr., *Sphagnum angustifolium* (Warnst.) C.E.O. Jensen, & *Sphagnum divinum* Flatberg & Hassel) on the permafrost peat plateau to sedges (*Carex* spp. and *Eriophorum* spp.) and very hydrophilic Sphagna (*Sphagnum riparium* Angstr. & *Sphagnum squarrosum* Crome) in the open (i.e., treeless) bog areas.

2.2 Study design

In 2008, we established 20 replicate plots in the permafrost peat plateau for long-term gas flux monitoring (Figure 1a). In 2017, we established 12 additional plots at the edge of an expanding collapse bog feature to study the impacts of active thermokarst (Figure 1b). Additional descriptions of the permafrost peat plateau and collapse bog features can be found in James *et al*., (2021); Manies *et al*., (2021); Waldrop *et al*., (2021). Each study plot consisted of a 1m x 1m vegetation sampling plot with a 60 x 60 cm gas flux collar inserted into the soil located in the center of each plot (Figure 2). In all cases, plots and flux collars were allowed to equilibrate in the soil for a minimum of two weeks prior to gas sampling. Further details are provided in methods sections below.

In 2018, we categorized our plot network into permafrost thaw zones based on variation in active layer thickness (ALT). Our ALT values were measured in a consistent marked location within each plot in the autumn prior to the onset of seasonal refreezing across all measurement years (see additional details below). We used ALT measurements to assign each plot in the network to one of four stages of permafrost thaw: Stable permafrost, Early thaw, Intermediate thaw, and Advanced/Stabilized thaw. The Stable permafrost stage had ALT within the recorded reference period (2008-2012) for the permafrost peat plateau (Kane *et al*., unpublished data). Mean ALT during this reference period was 46 ± 7 cm, while ALT thickness in the Stable permafrost stage in 2017 averaged 54 ± 8 cm. ALT in the Early, Intermediate, and Advanced thaw stages averaged 68 ± 9 cm, 83 ± 7 cm, and 110 ± 19 cm, respectively. Due to spatial constraints at the site our final design had an uneven number of plots per thaw stage, with the initial 20 permafrost peat plateau plots being subdivided into eight Stable permafrost plots and 12 Early thaw stage plots, while the 12 collapse bog margin plots were subdivided into four Intermediate thaw stage plots and eight Advanced thaw stage plots.

2.3 Plant community composition

The vegetative community was assessed annually at each study plot during peak productivity (mid-July) from 2017–2019. Vegetation within our 32 plots was visually assessed to determine their percent cover by functional group and species according to Johnson *et al*. (1995). Specifically, the area coverages by bryophytes, herbs, graminoids, shrubs, and tree seedlings were quantified at the species level. Lichen and bryophyte specimens that could not be identified in the field were collected and verified in the lab according to Vitt, Marsh, & Bovey (1988) (non-*Sphagnum* bryophytes), Lange (1982) (*Sphagnum* specimens), and Brodo, *et al*., (2001) (lichens, esp. *Cladonia* specimens). The plant species *Sphagnum magellanicum* sensu lato has recently been split into multiple species following Hassel *et al*. (2018). Voucher specimens previously identified as *Sphagnum magellanicum* were re-keyed out to *Sphagnum divinum* based on geographical range, leaf morphology, and hyalocyst pore size.

2.4 Greenhouse gas sampling

Greenhouse gas sampling was conducted every other week over the course of the growing season (late May to August) for three consecutive years (2017 to 2019), resulting in six to seven sampling events per year. Samples were collected using standard static chamber techniques (Carrol & Crill, 1997) following methods detailed by Chivers *et al*., (2009) and Olefeldt *et al*., (2017). Specifically, the 32 soil collars mentioned above were inserted permanently into the soil profile to a depth of 10 cm and equipped with foam tape to form an air-tight seal with the static chambers. We allowed for a settlement period of at least two weeks before gas flux data were collected on an installed soil collar. Clear chambers were built to interface with these soil collars, from 0.6 cm thick Lexan, with a final internal volume of 0.23 m^3, and equipped with two internal fans to mix air inside the chamber. Due to limitations in the size of the chambers, measured fluxes were reflective of activity in the understory plants, the ground layer, and surface soils, but respiration and uptake by larger statured woody plants could not be captured and were therefore excluded in our analysis. Prior to each sampling event, collars and chambers were checked for secure attachment and gas-tight seals.

Carbon dioxide (CO_2) fluxes were measured under ambient light and shrouded dark conditions to quantify net ecosystem exchange (NEE) and ecosystem respiration (ER) rates, respectively. During CO_2 flux measurements chambers were sealed for 2 to 3 min, with CO_2 concentrations quantified every 1.6 s using a daily calibrated Portable Photosynthesis (PP Systems) EGM-4 infrared gas analyzer connected directly to the static chambers. Temperature, relative humidity, and photosynthetically active radiation (PAR) were measured continuously during CO_2 flux measurements using PP (portable photosynthesis) Systems TRP-1 sensors installed inside chambers. The CO_2 flux rates (μmol CO_2 m^{-2} s^{-1}) were calculated as the slope of CO_2 headspace concentration over time, where negative values indicated CO_2 uptake by the ecosystem while positive values indicated CO_2 release. Using a mass balance approach, NEE and ER were used to calculate gross primary productivity (GPP) as GPP = NEE - ER. Methane flux rates were determined by sealing and shrouding the static chamber and collecting well-mixed headspace samples with clean 20 ml gas syringes in five-minute intervals for 30 minutes. These gas samples were then processed within the following 24 hours using a Varian 3900 gas

chromatograph with an FID detector with a HayeSep N column. Methane flux rates (µmol CH_4 $\cdot m^{-2} \cdot min^{-1}$) were calculated as the change in headspace methane concentration over time.

2.5 Environmental predictors

Each of our gas flux sampling events was accompanied by a suite of environmental measurements. At each plot, we measured temperature (°C) of the top 10 cm of soil with a temperature probe, soil moisture (mV, % moisture) within the top 5 cm with a Dynamax HH2 soil moisture probe, and seasonal depth-to-ice (cm) with a 120 cm metal tile probe. To get an estimate of ALT, we measured depth to refusal (top of near-surface permafrost) in late September each year at the time of maximum thaw (early fall) before onset of seasonal re-freezing at marked locations within each gas sampling plot. We relied on depth to refusal as our measure of active layer thickness because other approaches, such as electrical resistivity tomography (ERT) cause negative impacts to surface vegetation in these peatlands. Moreover, depth to refusal via frost probing campaigns allows us to compare our results to other long-term monitoring studies where frost probing is used in conjunction with permanent vegetation or gas flux plots.

2.6 Statistical analyses

Mixed effects models were used to evaluate whether ALT, methane flux, NEE, ER, and GPP significantly varied across the four classes of permafrost thaw stage and the three sampling years using the "nlme" package (Pinheiro *et al*., 2020) in R statistical analysis software. Methane flux and ER were transformed using Tukey Ladder of Powers in the "rcompanion" package (Mangiafico & Mangiafico, 2018) to ensure those models sufficed in meeting assumptions for residual heteroskedasticity and normality (CH_4: λ=0.075, ER: λ=0.075). ALT and GPP were left untransformed, as the distribution of residuals for these variables was not improved by the Tukey transformation. Plot ID was included as a random effect in our gas flux models to account for the repeated measures collected from the same collars over the three sample years.

Vegetation community data were used to create a dissimilarity matrix based on the Bray-Curtis dissimilarity index using the "vegan" package (Oksanen *et al*., 2019) in R. An analysis of similarities (ANOSIM) was used to assess differences in plant community composition between the four thaw stages. This ANOSIM was followed by a similarity percentages (SIMPER) analysis to quantify the dissimilarity in plant communities between each pairwise combination of treatment groups. We also used Ward's hierarchical cluster analysis to divide the plots into meaningful clusters based on plant community dissimilarity and to compare those clusters to our pre-defined thaw stage categories (R package "pvclust", Suzuki *et al*., 2019). The Bray-Curtis dissimilarity matrix was also used to generate a non-metric multidimensional scaling (NMDS) ordination to visually represent our multivariate plant community data. We chose NMDS over other ordination methods because unlike PCA and PCoA, NMDS does not assume a linear distribution of variables in the data matrix and is therefore less susceptible to the "horseshoe effect" (Palmer, 2004). In addition to the multivariate analysis of the plant communities, we also used linear mixed effects models to assess the fixed effects of permafrost thaw stages and

years on the abundance of key plant functional groups (ericoids, graminoids, and *Sphagnum* moss), as well as on overall plant species richness.

To identify specific plant taxa that could serve as indicators of the four thaw stages, we used indicator species analysis in the R package "indicspecies" using species abundance and frequency to calculate indicator values for individual plant species and species assemblages (pairs and trios) for each thaw stage treatment (de Caceres *et al*., 2020). This indicator value is a composite of two conditional probabilities: specificity, the probability that a surveyed plot belongs to the target treatment group given that the species or assemblage was present, and fidelity, the probability of finding that species or assemblage in plots of a given treatment group. We used multilevel pattern analysis (multipatt) to identify single species: single treatment group associations and single species: multiple treatment group associations. Additionally, we used the "indicators" function to identify species assemblages (singletons, pairs, and trios) as indicators for each treatment group, since some plant species may only co-occur in certain thaw stages. Species that appear in every plot for a given treatment were included as fixed elements. Using a standard alpha value of 0.05, some of our treatment groups had hundreds of valid indicator assemblages, so we further limited the candidate pool with the "pruneindicators" function using a specificity threshold of 0.8 and a fidelity threshold of 0.2. This function does three things with the candidate indicator pool. From the entire pool of valid indicators, it 1) discards species assemblages that are nested within other assemblages, 2) evaluates the percentage of sites within a treatment group covered by the remaining indicators, and 3) explores subsets of valid indicators until a subset is obtained with the same coverage as the full set of valid indicators.

3 Results

3.1 Active layer thickness (ALT)

Active layer thickening occurred over the three-year sampling period at all plots, suggesting gradual top-down permafrost thaw in all plots. Across thaw stages, mean ALT exceeded that of the reference period (2008-2012). However, the rate of active layer thickening varied by thaw stage (Figure 3). At the Stable thaw stage, mean ALT during the sampling period remained within the range of variation observed during the reference period (46 ± 8 cm), and ALT did not vary among sample years (Figure 2). In contrast, ALT increased during the sampling period in the Early, Intermediate, and Advanced thaw stages, and values exceeded that of the reference period, with ALT values of 78 ± 7, 99 ± 15, and 114 ± 12 cm, respectively. These measurements fell well outside the range of ALT observed during the reference period (Figure 3).

The change in ALT during the sampling period occurred faster in the Early and Intermediate stages than in the Stable and Advanced stages. As an example of how quickly thaw progressed through the site, we observed that by 2019 the ALT at the Intermediate thaw stage was approximately equal to ALT values at the Advanced thaw stage in 2017, while the ALT at Early thaw stage plots in 2019 resembled those at the Intermediate thaw stage in 2017. In contrast, there was minimal change in measured ALT at plots of the Advanced stage permafrost

thaw over the sampling period, but this likely was influenced by ALT often exceeding the length of the tile probe (120 cm).

3.2 Response of the plant community to thaw

We found multiple lines of evidence for a predictable progression in the plant community composition along our four thaw stages. The ANOSIM showed separation of plant communities among our four thaw stages (R=0.436, p=0.001, permutations=999). Quantifying these differences with SIMPER showed that, as expected, the greatest dissimilarity occurred between the Stable and Advanced thaw stages, and the least dissimilarity between sequential pairwise comparisons (i.e., Stable to Early, Early to Intermediate; Table 2), suggesting a linear progression through these transitional stages. The abundance matrix was used to generate an NMDS ordination plot (Figure 5). Plots cluster strongly based on thaw stage, and their organization in the ordination space again suggests a somewhat linear and sustained progression through the four thaw stages. This progression was consistent with a microclimate characterized by increasing soil moisture and soil temperature with advancing thaw stage, as indicated by vectors in the ordination plot.

During the sampling period, total plant species richness decreased with thaw stage ($F_{3,80}$=7.428, p=0.0002), but we found insufficient evidence to suggest an effect of sample year ($F_{2,80}$=0.981 p=0.379) or an interaction between these two effects ($F_{6,80}$=1.568, p=0.167; Figure 5a). There were substantial changes in key functional group abundance with thaw stage, but trends were unique to each group. Graminoid abundance varied by an interaction between thaw stage and year ($F_{6,80}$=2.514; p=0.0279), driven largely by a rapid, dramatic increase in graminoid abundance at the Intermediate thaw stage corresponding with lateral expansion of the active thaw margin over time. Mean graminoid abundance in this thaw stage increased from less than 25% in 2017 to greater than 60% in 2018 and greater than 90% in 2019 (Figure 5b). We found that ericoid abundance decreased linearly with advancing thaw stage ($F_{3,80}$=31.359; p<0.0001) and time ($F_{2,80}$=4.888; p=0.0099) with insufficient evidence for an interaction between time and thaw stage ($F_{6,80}$=1.191; p=0.3199) (Figure 5c). *Sphagnum* moss abundance increased slightly with advancing thaw stage ($F_{3,80}$=11.6065; p<0.0001), but showed a substantial drop at the Intermediate stage at the thaw margin, effectively mirroring the trend observed in graminoid abundance (Figure 5d).

Of the 62 plant species surveyed across our treatment sites, 22 showed strong preference for specific thaw stages (Table 2a). Indicator species analysis identified species combinations that served as reliable indicators for each thaw stage, as well as fixed elements (i.e., plant species that appeared in every plot) for three of the four thaw stage groups (Table 2b). Indicators for the Stable and Advanced thaw stages were intuitive, with taxa such as *Vaccinium uliginosum*, *Pleurozium schreberi*, and *Peltigera aphthosa* as indicators of the Stable permafrost stage, and *Sphagnum riparium* as the single most reliable indicator of the Advanced thaw stage. However, the results for the Early and Intermediate stages of thaw were more complex, with indicator assemblages spanning both forest taxa and bog taxa. For example, at the Early stage we saw as indicators an assemblage of plants more commonly associated with

bogs and fens in both the vascular layer (*Oxycoccus microcarpus*, *Chamaedaphne calyculata*, and *Drosera rotundifolia*) and the basal cryptogamic layer (*Sphagnum angustifolium*, *S. divinum*, and *S. warnstorfii*). The only reliable species pair at the Intermediate stage was *P. schreberi* and *S. riparium*, a forest moss and a bog moss respectively, further suggesting a rapid change in the microclimate conditions there, as it is rare for the two species to co-occur in a stable microclimate.

3.3 Soil CO_2 and CH_4 fluxes

Here we report chamber-based CO_2 and CH_4 emissions at peak productivity (mid-July) across the thaw stages during the three-year sampling period. Gas flux measurements showed that peak methane flux varied across permafrost thaw stage, but peak ecosystem respiration was comparatively unaffected. Methane fluxes increased with progressive thaw stages ($F_{3,13}$=9.51; p=0.0014) and varied by measurement year ($F_{2,56}$=5.01; p=0.0100), with no interaction between thaw stage and year ($F_{6,56}$=1.26; p=0.2887; Figure 6). The Stable thaw stage showed the lowest peak CH_4 flux rates. The Advanced thaw stage on average had the largest peak CH_4 fluxes. In general, peak CH_4 flux in the Early thaw stage was 270% greater than in the Stable permafrost stage and 1000% larger in the Advanced thaw stage than in the Stable permafrost stage. Averaged across our entire plot network, CH_4 emissions averaged 5.72±1.02 µmol $CH_4 \cdot m^{-2} \cdot min^{-1}$ in 2017, 10.27±2.12 µmol $CH_4 \cdot m^{-2} \cdot min^{-1}$ in 2018, and 9.26±1.88 µmol $CH_4 \cdot m^{-2} \cdot min^{-1}$ in 2019 (Figure 6).

In contrast to methane fluxes, CO_2 emissions were resilient to the effects of permafrost thaw, with minimal changes in ER, GPP, and NEE observed during the sampling period. ER did not vary between the thaw stages ($F_{3,13}$=1.15; p=0.3648), though the greatest mean ER fluxes tended to occur at the Stable permafrost stage while the smallest fluxes occurred at the Advanced thaw stage (Figure 7a). In general, differences in ER between thaw stages were smaller than for CH_4 fluxes, with a 15% decrease in ER from the Stable permafrost to Early thaw stage and a ~40% decrease from the Stable permafrost to Advanced thaw stage. Averaged across all thaw stages, there was a decrease in ER over time during the sampling period ($F_{2,56}$=3.21; p=0.0479), with no interaction between thaw stage and year ($F_{6,56}$=1.75; p=0.3983).

The greatest GPP fluxes occurred in Stable permafrost plots, with a gradual decrease in GPP with advancing stages of permafrost thaw ($F_{3,13}$=4.12, p=0.0295). There was no effect of sample year ($F_{2,56}$=2.04, p=0.1398) nor its interaction with thaw stage ($F_{6,56}$=0.974, p=0.4512) on GPP (Figure 7b). Our data showed no changes in NEE with thaw stage ($F_{3,13}$=1.06, p=0.3985), sample year ($F_{2,56}$=1.23, p=0.2996), or the interaction between thaw stage and sample year ($F_{6,56}$=0.353, p=0.9051) (Fig 6c).

4 Discussion

4.1 Detecting early-warning signs of permafrost thaw

The primary goal of this study was to assess whether changes in surface vegetation communities in a boreal peatland complex could be used to identify early onset of permafrost

thaw, as measured through active layer thickness (ALT). Our sampling design included variation in ALT across a spatial thaw gradient as well as surface permafrost thaw that occurred over time. Trends in ALT suggest relatively consistent patterns of gradual thaw across all of our plots since our reference period (2008-2012), with localized hotspots of abrupt thaw emerging over the last few years of sampling. There is no evidence of wildfire at our study site within at least the past 50 years, pointing towards ongoing warming as the likely leading cause of thaw. Additionally, the site has experienced increasing spring and summer precipitation since 2014, which may be contributing to accelerating thaw rates (Douglas *et al*., 2020; Euskirchen *et al*., 2020). Our results suggest predictable patterns of plant community changes in response to these changes in ALT. There was a linear progression from a ground layer dominated by forest-dwelling feather mosses to increasingly hydrophilic *Sphagnum* species. This was accompanied by shifts in the vascular understory from ericoids in the Stable permafrost area and Early thaw stage being replaced first by cottongrass (*Eriophorum* spp.) and finally by true sedges (*Carex* spp.) in the Intermediate and Advanced thaw stages. Our Indicator species analysis shows that *Eriophorum* spp. are the most reliable indicators of an expanding thaw front (i.e., shift from Early to Intermediate thaw stages) and development of thermokarst features. This finding is consistent with previous work, as *Eriophorum* spp. have long been cited as a good indicator of permafrost thaw across a wide range of the North American boreal forest (Camill, 1999; Beilman, 2001). It is worth noting that while *Eriophorum* spp. are quite common throughout the entire peatland complex, they completely dominate the understory at the Intermediate thaw stage, coinciding with lateral expansion of the active thaw front.

During the earliest stages of thaw, the understory remained ericoid-dominant, but became graminoid-dominant as thaw progressed further. Graminoid abundance had an inverse relationship with *Sphagnum* moss abundance, perhaps suggesting a competitive or inhibitory relationship. At the functional group level, we saw a progression from ericaceous shrubs and feather mosses to graminoids and *Sphagnum* mosses with increased active layer thickness, but there were also consistent patterns of species level turnover within functional groups. At the species level, we observed a consistent transition from bog blueberry (*Vaccinium uliginosum*), marsh Labrador tea (*Rhododenron tomentosum*) and cloudberry (*Rubus chamaemorus*) in the Stable permafrost areas to bog cranberry (*Vaccinium oxycoccos*), sundews (*Drosera rotundifolia*), and leatherleaf (*Chamaedaphne calyculata*) in the Early stages of thaw, and finally to cottongrasses (*Eriophorum* spp.) and sedges (*Carex* spp.) in the Advanced stages of thaw. In the ground layer, we saw a progression from feather mosses (*Hylocomium splendens*, *Pleurozium schreberi*, etc.) to *Sphagnum* mosses in areas undergoing thaw. Changes in *Sphagnum* moss species were the most reliable indicators of this earliest onset of permafrost thaw. We found that *Sphagnum fuscum* was a good indicator of areas in transition from Stable permafrost to Early thaw, *Sphagnum angustifolium*, *Sphagnum divinum*, and *Sphagnum warnstorfii* were good indicators of the transition from Early to Intermediate thaw, and *Sphagnum riparium* was the most reliable indicator of Advanced thaw. The trends we observed in species and functional group turnover are consistent with other studies from Alaska and western Canada, suggesting these indicators may be useful for much of the permafrost peatlands of the North American boreal region (Camill, 1999; Beilman, 2001; Olefeldt *et al*., 2013). Interestingly, the patterns we found suggest a community-level progression from forest-

like (black spruce and feather mosses) to bog-like (ericaceous shrubs and *Sphagnum* mosses) to fen-like (*Carex* spp. and *Sphagnum riparium*) as the active layer thickens and we move through the stages of thaw.

In terms of application and utility, Early thaw onset vegetation indicators like bog cranberry (*Vaccinium oxycoccos*), leatherleaf (*Chamaedaphne calyculata*), and our array of *Sphagnum* mosses will be useful for monitoring change in northern ecosystems and may also have utility for remote sensing efforts, particularly for measurements that can track moss species with differing affinity for wet conditions. Previous studies have utilized the moss layer to monitor land cover change in arctic tundra and boreal forest areas, however most of this work has been conducted at the functional group or guild level, rather than the level of individual genera or species (Bubier *et al*., 1997; Stow *et al*., 2004; Cerrejón *et al*., 2020). There are perceptible differences, even to the naked eye, in the color of our reported indicator taxa, even between closely related taxa, such as the *Sphagnum* mosses. Therefore, it is likely that the spectral response patterns of these plants may have some utility when applied to airborne or satellite-based imagery. While remote sensed imagery, such as from the Sentinel-2 satellite system, recently has been used to detect thawed and subsided areas in northern peatlands (Gibson *et al*., 2021), these methods have not yet been used to identify more subtle vegetation changes that occur during early onset of thaw.

4.2 Carbon cycle responses to early onset of thaw versus later stages of thermokarst development

The earliest stages of active layer thickening are associated with enhanced carbon fluxes as methane. Relative to the Stable thaw stage, the Early thaw stage experienced a five-fold increase in methane emissions despite only minor changes in ALT. These early-thaw methane emissions account for roughly 30% of the total increased methane output over the full forest-to-bog transition. Thaw initiated near the bog edges (Advanced thaw) ~150 years ago (Manies *et al*., 2021). Thus, despite only representing ~10% of the thaw progression timeline, methane emissions during the first decade of thaw account for nearly one-third of the total increase in methane emissions. Increases in methane emission were not accompanied by a commensurate change in CO_2 emissions, which altered CO_2:CH_4 ratios across the thaw stages. These results imply that areas undergoing early thaw may have a much greater warming potential than previously recognized. Taken together, our study clearly shows microclimate and carbon emissions respond quickly to active layer thickening even before thermokarst features become apparent in peatlands.

In addition to the increased methane emissions with progressive thaw stage, we saw site-wide increases in methane production throughout the sampling period, regardless of thaw status. This may be an outcome of top-down thaw occuring in warming permafrost soils globally (Biskaborn *et al*., 2019), intensified by the thermal impacts of rainwater on permafrost during the wetter than average growing seasons during our sampling period (Neumann *et al*. 2019, Douglas *et al*. 2020, Mekonnen *et al*. 2021, Euskirchen, *et al*., 2020).

Increased methane emissions coincided with shifts in local belowground environmental conditions and plant community composition along the thaw gradient. Soil moisture content and temperature, both known to promote methanogenesis (Bubier & Moore, 1994; Wang *et al*., 1996), increased with the advancing thaw stages. These same environmental conditions supported increasing graminoid abundance and declining ericoid abundance. The combination of wetter, warmer surface soils and increased graminoids with labile root exudates likely contributed to increasing methane emissions by stimulating methane production and transport, while suppressing methane oxidation (Turner *et al*., 2020). Conversely, the presence of sedges with their characteristic aerenchymous tissues can have an oxidizing effect on the rhizosphere, reducing overall methane emissions by facilitating methane oxidation (Rupp *et al*., 2019, Kane *et al*., 2019). While this oxidizing influence limits potential methane output, wet, sedge-dominant areas in peatlands remain a net methane source (Rupp *et al*., 2019).

The Advanced thaw stage was associated with high methane flux and a greater abundance of *Sphagnum* mosses, particularly *Sphagnum riparium*. Despite this relationship, many *Sphagnum* species are known to have syntrophic associations with methanotrophic bacteria, with 10 – 30% of *Sphagnum* biomass carbon sourced from microbially mediated methane oxidation (Larmola *et al*., 2010). All the *Sphagnum* species that occur at our permafrost thaw sites show some level of methanotrophy that varies with water table depth (Larmola *et al*., 2010). This suggests *Sphagnum* moss dominance in the Advanced thaw stage may have helped in mitigating overall thaw-driven methane emissions from this landscape and methane losses could be greater in their absence.

Despite significant shifts in both vegetation community and active layer thickness, CO_2 fluxes remained resilient to changes in ALT. However, our measurements did not include two major components of peatland CO_2 fluxes. First, our flux chambers are too small to encompass trees. There is a clear progression from healthy black spruce in the Stable stage to stressed trees with significantly fewer needles in the Early stage, to dead and dying trees in the Advanced stage. Thus, there is likely a major decline in tree productivity and associated carbon uptake with progressive thaw that we are unable to capture. Second, we report growing season carbon fluxes. Shoulder season and winter flux rates are smaller than those of the growing season, but account for a substantial pool of carbon emissions (Natali *et al*., 2019).

Our results show cumulative changes in carbon emissions with permafrost thaw similar to those reported in the literature (Heffernan *et al*., 2020), with the greatest C emissions (CH_4 + CO_2) in the later stages of thaw (Olefeldt *et al*., 2013). Across all thaw stages, C losses averaged 20.2±7.2 g $C \cdot m^{-2} \cdot yr^{-1}$ (excluding winter fluxes), falling within the wide range of 27.3 g $C \cdot m^{-2} \cdot yr^{-1}$ of uptake to 106.6 g $C \cdot m^{-2} \cdot yr^{-1}$ of losses reported by Heffernan *et al*. (2020). The Stable stage at our site has C stocks of ~38 kg C m^{-2} (Manies *et al*., 2021); thus, our results account for <1% loss of estimated permafrost peat carbon stocks per year during early thaw. These fluxes overall are smaller than those reported by Jones *et al*. (2016), who concluded that ~30% of permafrost peat C stocks were lost in the first few decades following thaw. Our flux-based estimates of peat C loss (0.02 kg C $m^{-2} \cdot yr^{-1}$) are within an order of magnitude of C losses for their youngest thaw bogs (<0.5 kg C $m^{-2} \cdot yr^{-1}$) but are much smaller than the reported C losses from older thaw

bogs (3.5 kg C m^{-2}·yr^{-1}; Jones *et al*., 2016). Permafrost history, more specifically the age of permafrost formation in relation to the timing of peat formation, controls the fate of permafrost C upon thaw (Manies *et al*., 2021) and likely explains some of these discrepancies between our results and previous studies. Despite the relatively low C losses we observed in comparison with previous research, our flux partitioning approach allows us to show that the change in C emissions during early thaw may be more of a qualitative shift (CH_4 rather than CO_2) than a quantitative one.

We upscaled our results using estimates of the global area of early or active thaw in peatland environments (Turetsky *et al*., 2020). Interpolating from our growing season flux data, we estimated an annual flux of 7.4 g CH_4 m^{-2}·yr^{-1} in the Early thaw stage and multiplied this flux estimate by an estimated 1.05 million km^2 of lowland organic (wetland) areas in the northern permafrost region undergoing active thaw (Turetsky *et al*., 2020). If the trends observed in this study are generalizable to other lowland organic (i.e., peatland-rich) thermokarst landscapes globally, our results suggest that up to 7.8 Tg CH_4 per year could be released during early-onset permafrost peatland thaw (prior to the onset of visible thermokarst collapse bog formation). While we acknowledge that this should be treated as a very rough estimate, it is also conservative as it does not include CH_4 emissions during shoulder and winter seasons. Our estimate of CH_4 flux associated with early-onset permafrost thaw in northern peatlands represents ~5% of global wetland methane emissions and is comparable in magnitude to recent increases that have been called an “exceptional surge” in global wetland methane emissions (Zhang *et al*., 2023). With the stronger radiative forcing of methane relative to CO_2, our results provide ample motivation to examine the contribution of early-stage permafrost thaw in northern peatlands across other environmental settings and regions.

Acknowledgments

The authors would like to acknowledge the assistance of the Fairbanks USGS office, the Bonanza Creek Long Term Ecological Research network (LTER), and the University of Alaska, Fairbanks, without which this work would not be possible. We would also like to thank USGS research scientist Mark Waldrop, Bonanza Creek site manager Jamie Hollingsworth, and the members of the Alaskan Peatland Experiment (APEX) field crew during the sampling period: Elle Barton, Kristen Bill, Morgan Brown, Devan Bruce, Emilia Grzesik, Danielle Rupp, and Evan Schijns.

T. Douglas acknowledges the Department of Defense's Strategic Environmental Research and Development Program (project RC18-1170) and Environmental Science and Technology Certification Program (RC22-7408). C.M. Dieleman acknowledges the National Science Engineer Research Council Postdoctoral fellowship program. This project was funded by National Science Foundation grants DEB LTREB-1354370. The APEX site also has been supported by National Science Foundation Grants DEB-0425328, DEB-0724514 and DEB-0830997. The Bonanza Creek LTER program was funded jointly by NSF Grant DEB-0620579 and a USDA Forest Service Pacific Northwest Research Grant PNW01-JV11261952-231. E. Kane acknowledges in-kind support from the U.S.D.A. Forest Service, Northern Research Station (Houghton, Michigan, USA).

Open Research

All data used for analyses in this study are publicly available. Master data files are archived at the Bonanza Creek LTER data catalog accessible via DOI: 10.6073/pasta/f3d08b259b48cb8c3999c2c5de3b8358, 10.6073/pasta/5dcbedef3b239a3b5a191e2ec7dd5b91, and 10.6073/pasta/03b90d16733715444e2a61e28a96517c. Trimmed data frames and R code used in the analyses is archived at 10.5281/zenodo.14201152. For further details, please contact the corresponding author.

References

Albano, L. J., Turetsky, M. R., Mack, M. C., & Kane, E. S. (2021). Deep roots of Carex aquatilis have greater ammonium uptake capacity than shallow roots in peatlands following permafrost thaw. *Plant and Soil*, *465*, 261-272.

Beilman, D. W. (2001). Plant community and diversity change due to localized permafrost dynamics in bogs of western Canada. *Canadian Journal of Botany*, *79*(8), 983-993.

Beilman, D. W., & Robinson, S. D. (2003, July). Peatland permafrost thaw and landform type along a climatic gradient. In *Proceedings of the 8th International Conference on Permafrost* (Vol. 1, pp. 61-65). Zurich: Balkema.

Biskaborn, B. K., Smith, S. L., Noetzli, J., Matthes, H., Vieira, G., Streletskiy, D. A., ... & Lantuit, H. (2019). Permafrost is warming at a global scale. *Nature communications*, *10*(1), 264.

Brodo, I. M., Sharnoff, S. D., & Sharnoff, S. (2001). *Lichens of north America*. Yale University Press.

Bubier, J. L., & Moore, T. R. (1994). An ecological perspective on methane emissions from northern wetlands. *Trends in ecology & evolution*, *9*(12), 460-464.

Bubier, J. L., Rock, B. N., & Crill, P. M. (1997). Spectral reflectance measurements of boreal wetland and forest mosses. *Journal of Geophysical Research: Atmospheres*, *102*(D24), 29483-29494.

Camill, P. (1999). Patterns of boreal permafrost peatland vegetation across environmental gradients sensitive to climate warming. *canadian Journal of Botany*, *77*(5), 721-733.

Camill, P. (2005). Permafrost thaw accelerates in boreal peatlands during late-20th century climate warming. *Climatic Change*, *68*(1), 135-152.

Carroll, P., & Crill, P. (1997). Carbon balance of a temperate poor fen. *Global Biogeochemical Cycles*, *11*(3), 349-356.

Cerrejón, C., Valeria, O., Mansuy, N., Barbé, M., & Fenton, N. J. (2020). Predictive mapping of bryophyte richness patterns in boreal forests using species distribution models and remote sensing data. *Ecological Indicators*, *119*, 106826.

Chacho, E. F., Arcone, S. A., & Delaney, A. J. (1995). *Bair Lakes Target Facility Permafrost and Groundwater Study*. US Army Cold Regions Research and Engineering Laboratory.

Chivers, M. R., Turetsky, M. R., Waddington, J. M., Harden, J. W., & McGuire, A. D. (2009). Effects of experimental water table and temperature manipulations on ecosystem CO 2 fluxes in an Alaskan rich fen. *Ecosystems*, *12*, 1329-1342.

Cox, W.D. wico2646. (2024). wico2646/APEX-Storage: APEX beta early thaw data v1.0.0 (v1.0.0-beta-thaw). Zenodo. https://doi.org/10.5281/zenodo.14201152

De Caceres, M., Jansen, F., & De Caceres, M. M. (2016). Package 'indicspecies'. *indicators*, *8*(1).

Dieleman, C. M., Branfireun, B. A., McLaughlin, J. W., & Lindo, Z. (2016). Enhanced carbon release under future climate conditions in a peatland mesocosm experiment: the role of phenolic compounds. *Plant and Soil*, *400*, 81-91.

Dieleman, C. M., Day, N. J., Holloway, J. E., Baltzer, J., Douglas, T. A., & Turetsky, M. R. (2022). Carbon and nitrogen cycling dynamics following permafrost thaw in the Northwest Territories, Canada. *Science of the Total Environment*, *845*, 157288.

Douglas, T. A., Turetsky, M. R., & Koven, C. D. (2020). Increased rainfall stimulates permafrost thaw across a variety of Interior Alaskan boreal ecosystems. *NPJ Climate and Atmospheric Science*, *3*(1), 28.

Douglas, T. A., Hiemstra, C. A., Anderson, J. E., Barbato, R. A., Bjella, K. L., Deeb, E. J., ... & Wagner, A. M. (2021). Recent degradation of interior Alaska permafrost mapped with ground surveys, geophysics, deep drilling, and repeat airborne lidar. *The Cryosphere*, *15*(8), 3555-3575.

Euskirchen, E. S., Edgar, C. W., Kane, E. S., Waldrop, M. P., Neumann, R. B., Manies, K. L., ... & Turetsky, M. R. (2024). Persistent net release of carbon dioxide and methane from an Alaskan lowland boreal peatland complex. *Global Change Biology*, *30*(1), e17139.

Frego, K. A. (2007). Bryophytes as potential indicators of forest integrity. *Forest ecology and management*, *242*(1), 65-75.

Frolking, S., Roulet, N. T., Tuittila, E., Bubier, J. L., Quillet, A., Talbot, J., & Richard, P. J. H. (2010). A new model of Holocene peatland net primary production, decomposition, water balance, and peat accumulation. *Earth System Dynamics*, *1*(1), 1-21.

Gibson, C., Cottenie, K., Gingras-Hill, T., Kokelj, S. V., Baltzer, J. L., Chasmer, L., & Turetsky, M. R. (2021). Mapping and understanding the vulnerability of northern peatlands to permafrost thaw at scales relevant to community adaptation planning. *Environmental Research Letters*, *16*(5), 055022.

Hassel, K., Kyrkjeeide, M. O., Yousefi, N., Prestø, T., Stenøien, H. K., Shaw, J. A., & Flatberg, K. I. (2018). Sphagnum divinum (sp. nov.) and S. medium Limpr. and their relationship to S. magellanicum Brid. *Journal of Bryology*, *40*(3), 197-222.

Heffernan, L., Estop-Aragonés, C., Knorr, K. H., Talbot, J., & Olefeldt, D. (2020). Long-term impacts of permafrost thaw on carbon storage in peatlands: Deep losses offset by surficial accumulation. *Journal of Geophysical Research: Biogeosciences*, *125*(3), e2019JG005501.

Hugelius, G., Strauss, J., Zubrzycki, S., Harden, J. W., Schuur, E. A., Ping, C. L., ... & Kuhry, P. (2014). Estimated stocks of circumpolar permafrost carbon with quantified uncertainty ranges and identified data gaps. *Biogeosciences*, *11*(23), 6573-6593.

Hugelius, G., Loisel, J., Chadburn, S., Jackson, R. B., Jones, M., MacDonald, G., ... & Yu, Z. (2020). Large stocks of peatland carbon and nitrogen are vulnerable to permafrost thaw. *Proceedings of the National Academy of Sciences*, *117*(34), 20438-20446.

Hylander, K. (2009). No increase in colonization rate of boreal bryophytes close to propagule sources. *Ecology*, *90*(1), 160-169.

James, S. R., Minsley, B. J., McFarland, J. W., Euskirchen, E. S., Edgar, C. W., & Waldrop, M. P. (2021). The biophysical role of water and ice within permafrost nearing collapse: Insights from novel geophysical observations. *Journal of Geophysical Research: Earth Surface*, *126*(6), e2021JF006104.

Johnson, D., Kershaw, L., & MacKinnon, A. (1995). Jim Pojar, Plants of the Western Boreal Forest and Aspen Parkland. *Vancouver, Canada: Lone Pine Publishing*.

Johnstone, J. F., Allen, C. D., Franklin, J. F., Frelich, L. E., Harvey, B. J., Higuera, P. E., ... & Turner, M. G. (2016). Changing disturbance regimes, ecological memory, and forest resilience. *Frontiers in Ecology and the Environment*, *14*(7), 369-378.

Jones, M. C., Booth, R. K., Yu, Z., & Ferry, P. (2013). A 2200-year record of permafrost dynamics and carbon cycling in a collapse-scar bog, interior Alaska. *Ecosystems*, *16*, 1-19.

Jones, M. C., Harden, J., O'Donnell, J., Manies, K., Jorgenson, T., Treat, C., & Ewing, S. (2017). Rapid carbon loss and slow recovery following permafrost thaw in boreal peatlands. *Global change biology*, *23*(3), 1109-1127.

Jorgenson, M. T., Douglas, T. A., Liljedahl, A. K., Roth, J. E., Cater, T. C., Davis, W. A., ... & Racine, C. H. (2020). The roles of climate extremes, ecological succession, and hydrology in repeated permafrost aggradation and degradation in fens on the Tanana Flats, Alaska. *Journal of Geophysical Research: Biogeosciences*, *125*(12), e2020JG005824.

Lange, B. (1982). Key to northern boreal and arctic species of Sphagnum, based on characteristics of the stem leaves.

Larmola, T., Tuittila, E. S., Tiirola, M., Nykänen, H., Martikainen, P. J., Yrjälä, K., ... & Fritze, H. (2010). The role of Sphagnum mosses in the methane cycling of a boreal mire. *Ecology*, *91*(8), 2356-2365.

Mangiafico, S., & Mangiafico, M. S. (2017). Package 'rcompanion'. *Cran Repos*, *20*, 1-71.

Manies, K. L., Jones, M. C., Waldrop, M. P., Leewis, M. C., Fuller, C., Cornman, R. S., & Hoefke, K. (2021). Influence of permafrost type and site history on losses of permafrost carbon after thaw. *Journal of Geophysical Research: Biogeosciences*, *126*(11), e2021JG006396.

McGuire, A. D., Lawrence, D. M., Koven, C., Clein, J. S., Burke, E., Chen, G., ... & Zhuang, Q. (2018). Dependence of the evolution of carbon dynamics in the northern permafrost region on the trajectory of climate change. *Proceedings of the National Academy of Sciences*, *115*(15), 3882-3887.

Mekonnen, Z. A., Riley, W. J., Grant, R. F., & Romanovsky, V. E. (2021). Changes in precipitation and air temperature contribute comparably to permafrost degradation in a warmer climate. *Environmental Research Letters*, *16*(2), 024008.

Natali, S. M., Watts, J. D., Rogers, B. M., Potter, S., Ludwig, S. M., Selbmann, A. K., ... & Zona, D. (2019). Large loss of CO2 in winter observed across the northern permafrost region. *Nature Climate Change*, *9*(11), 852-857.

Neumann, R. B., Moorberg, C. J., Lundquist, J. D., Turner, J. C., Waldrop, M. P., McFarland, J. W., ... & Turetsky, M. R. (2019). Warming effects of spring rainfall increase methane emissions from thawing permafrost. *Geophysical Research Letters*, *46*(3), 1393-1401.

Nisbet, R. E. R., Fisher, R., Nimmo, R. H., Bendall, D. S., Crill, P. M., Gallego-Sala, A. V., ... & Nisbet, E. G. (2009). Emission of methane from plants. *Proceedings of the Royal Society B: Biological Sciences*, *276*(1660), 1347-1354.

O'Donnell, J. A., Jorgenson, M. T., Harden, J. W., McGuire, A. D., Kanevskiy, M. Z., & Wickland, K. P. (2012). The effects of permafrost thaw on soil hydrologic, thermal, and carbon dynamics in an Alaskan peatland. *Ecosystems*, *15*, 213-229.

Oksanen, J., Blanchet, F. G., Kindt, R., Legendre, P., Minchin, P. R., O'hara, R. B., ... & Oksanen, M. J. (2013). Package 'vegan'. *Community ecology package, version*, *2*(9), 1-295.

Olefeldt, D., Turetsky, M. R., Crill, P. M., & McGuire, A. D. (2013). Environmental and physical controls on northern terrestrial methane emissions across permafrost zones. *Global change biology*, *19*(2), 589-603.

Olefeldt, D., Euskirchen, E. S., Harden, J., Kane, E., McGuire, A. D., Waldrop, M. P., & Turetsky, M. R. (2017). A decade of boreal rich fen greenhouse gas fluxes in response to natural and experimental water table variability. *Global change biology*, *23*(6), 2428-2440.

Osterkamp, T. E., Jorgenson, M. T., Schuur, E. A. G., Shur, Y. L., Kanevskiy, M. Z., Vogel, J. G., & Tumskoy, V. E. (2009). Physical and ecological changes associated with warming permafrost and thermokarst in interior Alaska. *Permafrost and Periglacial Processes*, *20*(3), 235-256.

Palmer, M. W. (2004). Ordination Methods-an overview. *Botany Department, Oklahoma State University, Stillwater, Oklahoma*, *74078*.

Patiño, J., & Vanderpoorten, A. (2018). Bryophyte biogeography. *Critical Reviews in Plant Sciences*, *37*(2-3), 175-209.

Pinheiro, J., Bates, D., DebRoy, S., Sarkar, D., Heisterkamp, S., Van Willigen, B., & Maintainer, R. (2017). Package 'nlme'. *Linear and nonlinear mixed effects models, version*, *3*(1), 274.

Ratajczak, Z., Carpenter, S. R., Ives, A. R., Kucharik, C. J., Ramiadantsoa, T., Stegner, M. A., ... & Turner, M. G. (2018). Abrupt change in ecological systems: inference and diagnosis. *Trends in Ecology & Evolution*, *33*(7), 513-526.

Rupp, D., Kane, E. S., Dieleman, C., Keller, J. K., & Turetsky, M. (2019). Plant functional group effects on peat carbon cycling in a boreal rich fen. *Biogeochemistry*, *144*, 305-327.

Rupp, D. L., Lamit, L. J., Techtmann, S. M., Kane, E. S., Lilleskov, E. A., & Turetsky, M. R. (2021). The rhizosphere responds: Rich fen peat and root microbial ecology after long-term water table manipulation. *Applied and Environmental Microbiology*, *87*(12), e00241-21.

Salmon, V. G., Soucy, P., Mauritz, M., Celis, G., Natali, S. M., Mack, M. C., & Schuur, E. A. (2016). Nitrogen availability increases in a tundra ecosystem during five years of experimental permafrost thaw. *Global Change Biology*, *22*(5), 1927-1941.

Salmon, V. G., Schädel, C., Bracho, R., Pegoraro, E., Celis, G., Mauritz, M., ... & Schuur, E. A. (2018). Adding depth to our understanding of nitrogen dynamics in permafrost soils. *Journal of Geophysical Research: Biogeosciences*, *123*(8), 2497-2512.

Schädel, C., Bader, M. K. F., Schuur, E. A., Biasi, C., Bracho, R., Čapek, P., ... & Wickland, K. P. (2016). Potential carbon emissions dominated by carbon dioxide from thawed permafrost soils. *Nature climate change*, *6*(10), 950-953.

Schuur, E. A., Bockheim, J., Canadell, J. G., Euskirchen, E., Field, C. B., Goryachkin, S. V., ... & Zimov, S. A. (2008). Vulnerability of permafrost carbon to climate change: Implications for the global carbon cycle. *BioScience*, *58*(8), 701-714.

Schuur, E. A., McGuire, A. D., Schädel, C., Grosse, G., Harden, J. W., Hayes, D. J., ... & Vonk, J. E. (2015). Climate change and the permafrost carbon feedback. *Nature*, *520*(7546), 171-179.

Stewart, K. J., & Mallik, A. U. (2006). Bryophyte responses to microclimatic edge effects across riparian buffers. *Ecological applications*, *16*(4), 1474-1486.

Stow, D. A., Hope, A., McGuire, D., Verbyla, D., Gamon, J., Huemmrich, F., ... & Myneni, R. (2004). Remote sensing of vegetation and land-cover change in Arctic Tundra Ecosystems. *Remote sensing of environment*, *89*(3), 281-308.

Suzuki, R., Terada, Y., Shimodaira, H., & Suzuki, M. R. (2019). Package 'pvclust'. *R Package. Hierarchical Clustering with P-Values via Multiscale Bootstrap Resampling. Version*, 2-2.

Turetsky, M. R., Mack, M. C., Hollingsworth, T. N., & Harden, J. W. (2010). The role of mosses in ecosystem succession and function in Alaska's boreal forest. *Canadian Journal of Forest Research*, *40*(7), 1237-1264.

Turetsky, M. R., Abbott, B. W., Jones, M. C., Anthony, K. W., Olefeldt, D., Schuur, E. A., ... & McGuire, A. D. (2020). Carbon release through abrupt permafrost thaw. *Nature Geoscience*, *13*(2), 138-143.

Turetsky, M.R., C.M. Dieleman, W.D. Cox, and Bonanza Creek LTER. 2024. APEX beta vegetation surveys from both the permafrost plateau area and the active thaw margin, from 2017 to present ver 2. Environmental Data Initiative. https://doi.org/10.6073/pasta/f3d08b259b48cb8c3999c2c5de3b8358 (Accessed 2024-11-21).

Turetsky, M.R., C.M. Dieleman, W.D. Cox, and Bonanza Creek LTER. 2024. APEX beta environmentals from both the permafrost plateau area and the active thaw margin, from 2017 to 2019 ver 2. Environmental Data Initiative. https://doi.org/10.6073/pasta/5dcbedef3b239a3b5a191e2ec7dd5b91 (Accessed 2024-11-21).

Turetsky, M.R., C.M. Dieleman, W.D. Cox, and Bonanza Creek LTER. 2024. APEX beta greenhouse gas flux data from both the permafrost plateau area and the active thaw margin, from 2017 on ver 2. Environmental Data Initiative. https://doi.org/10.6073/pasta/03b90d16733715444e2a61e28a96517c (Accessed 2024-11-21).

Turner, J. C., Moorberg, C. J., Wong, A., Shea, K., Waldrop, M. P., Turetsky, M. R., & Neumann, R. B. (2020). Getting to the root of plant-mediated methane emissions and oxidation in a thermokarst bog. *Journal of Geophysical Research: Biogeosciences*, *125*(11), e2020JG005825.

Van Breemen, N. (1995). How Sphagnum bogs down other plants. *Trends in ecology & evolution*, *10*(7), 270-275.

Vitt, D. H., Marsh, J. E., & Bovey, R. B. (1988). Mosses, lichens & ferns of northwest North America. *Lone Pine Publishing*.

Waldrop, M. P., W McFarland, J., Manies, K. L., Leewis, M. C., Blazewicz, S. J., Jones, M. C., ... & Cable, W. L. (2021). Carbon fluxes and microbial activities from boreal peatlands experiencing permafrost thaw. *Journal of Geophysical Research: Biogeosciences*, *126*(3), e2020JG005869.

Wang, Z., Zeng, D., & Patrick, W. H. (1996). Methane emissions from natural wetlands. *Environmental Monitoring and Assessment*, *42*, 143-161.

Yang, Z. P., Ou, Y. H., Xu, X. L., Zhao, L., Song, M. H., & Zhou, C. P. (2010). Effects of permafrost degradation on ecosystems. *Acta Ecologica Sinica*, *30*(1), 33-39.

Zhang, Z., Poulter, B., Feldman, A. F., Ying, Q., Ciais, P., Peng, S., & Li, X. (2023). Recent intensification of wetland methane feedback. *Nature Climate Change*, *13*(5), 430-433.

Table 1. Pairwise SIMPER (similarity percentage) comparison of plant communities of the four thaw stages. Note that percentages here refer to percent dissimilarity, where 0% would indicate identical communities and 100% would indicate communities with no shared members.

SIMPER	Stable	Early	Intermediate	Advanced
Stable	-	60.4%	70.4%	82.6%
Early	60.4%	-	69.6%	77.5%
Intermediate	70.4%	69.6%	-	75.3%
Advanced	82.6%	77.5%	75.3%	-

Table 2. Species identified through multilevel pattern analyses and indicator species analyses to be associated significantly more than by chance with single and multiple strata (thaw stage). Numbers are indicator values (generated by the package "indicspecies" in R) and *p*-values (in parenthesis). *Note that this refers to *Picea mariana* seedlings. Mature trees were not considered in this analysis.

a) Single species: multiple strata

Species	IndVal(p)	Stable	Early	Intermediate	Advanced
Betula glandulosa	0.585(0.001)	+			
Hylocomium splendens	0.569(0.002)	+			
Sphagnum capilifolium	0.435(0.031)	+			
Rhododendron tomentosum	0.959(0.001)	+	+		
Vaccinium uliginosum	0.931(0.001)	+	+		
*Picea mariana**	0.544(0.003)	+	+		
Sphagnum fuscum	0.500(0.010)	+	+		
Vaccinium oxycoccos	0.757(0.009)		+		
Rubus chamaemorus	0.978(0.001)	+	+	+	
Vaccinium vitis-idaea	0.949(0.001)	+	+	+	
Sphagnum angustifolium	0.729(0.025)	+	+	+	
Dicranum undulatum	0.538(0.049)	+	+	+	
Pleurozium schreberi	0.775(0.001)	+		+	
Peltigera aphthosa	0.527(0.004)	+		+	
Drosera rotundifolia	0.789(0.001)	+	+		+
Ptilium crista-castrensis	0.531(0.001)			+	
Eriophorum vaginatum	0.408(0.017)			+	
Chamaedaphne calyculata	0.922(0.001)		+	+	+
Sphagnum riparium	0.855(0.001)				+
Carex chordorrhiza	0.641(0.001)				+
Carex aquatilis	0.540(0.003)				+

b) Multiple species: single stratum.

Stable: Valid combinations 175, Coverage 75%	
Fixed elements (FE):	
Rhododendron tomentosum, Rubus chamaemorus, Vaccinium vitis-idaea	
Pruned indicators:	sqrtIV(p-value)
FE + *Pleurozium schreberi* +*Vaccinium uliginosum*	0.717(0.005)
FE + *Peltigera aphthosa*	0.447(0.005)
FE + *Dicranum undulatum* + *Tomenthypnum nitens*	0.427(0.010)
Early: Valid combinations 292, Coverage 94.4%	
Fixed elements (FE): *Rubus chamaemorus*	
Pruned indicators:	sqrtIV(p-value)
FE + *Vaccinium oxycoccos*	0.774(0.005)
FE + *Chamaedaphne calyculata* + *Drosera rotundifolia* +	0.703(0.005)
Sphagnum angustifolium	
FE + *Sphagnum divinum* + *Sphagnum warnstorfii*	0.609(0.005)
Intermediate: Valid combinations 53, Coverage 33.3%	
Fixed Elements (FE): *Chamaedaphne calyculata*	
Pruned indicators:	sqrtIV(p-value)
FE + *Pleurozium schreberi* + *Sphagnum riparium*	0.516(0.015)
Advanced: Valid combinations 110, Coverage 79.2%	
Fixed Elements (FE): none	
Pruned indicators:	sqrtIV(p-value)
Sphagnum riparium	0.871(0.005)

Figure 1a. Permafrost peat plateau area containing Stable and Early thaw stage plots. Photo by Evan Schijns 2018.

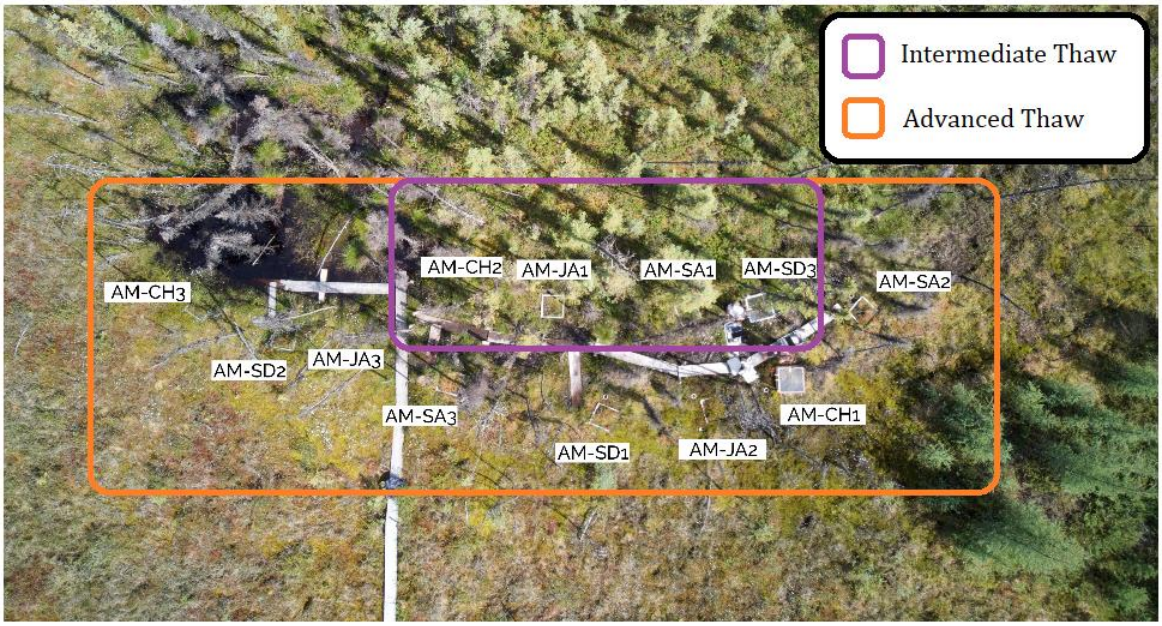

Figure 1b. Active thaw margin area containing Intermediate and Advanced thaw stage plots on either side of the thaw margin. Photo by Evan Schijns 2018.

Figure 2. Example plot photos showing soil collars inserted into the ground layer. The four plots shown are representative of the four thaw stages: a) Stable permafrost, b) Early thaw, c) Intermediate thaw, and d) Advanced thaw.

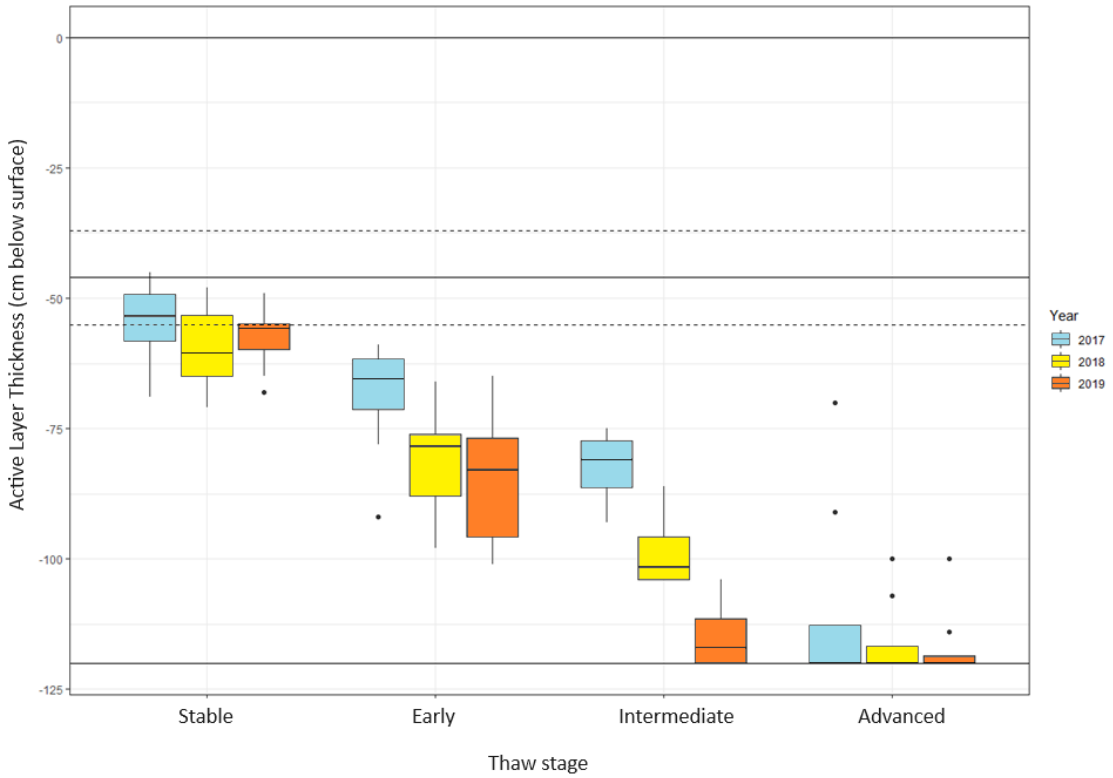

Figure 3. Active layer thickness (measured in late September) over three years across four thaw stage treatments. Reference period measurements taken from 2008-2012, with mean active layer thickness as a solid line (46cm below surface) with SD as dashed lines. Surface depth (0cm) and length of tile probe (120cm below surface) also represented as solid lines.

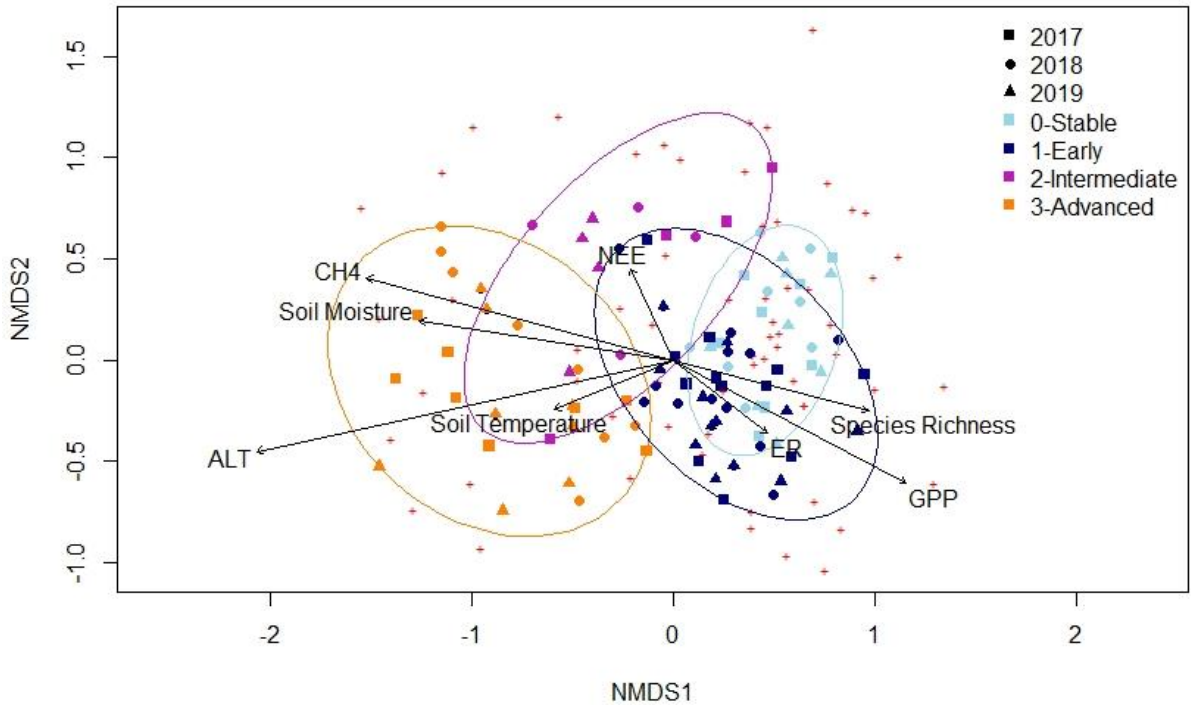

Figure 4. NMDS representation of 32 vegetation plots across the four stages of thaw (defined by variation in active layer thickness) and over three sampling years, with measured environmental variables as vectors in ordination space. Gas flux measures (CH_4, ER, GPP, NEE) included as vectors to show relationships with environmental factors and plant communities.

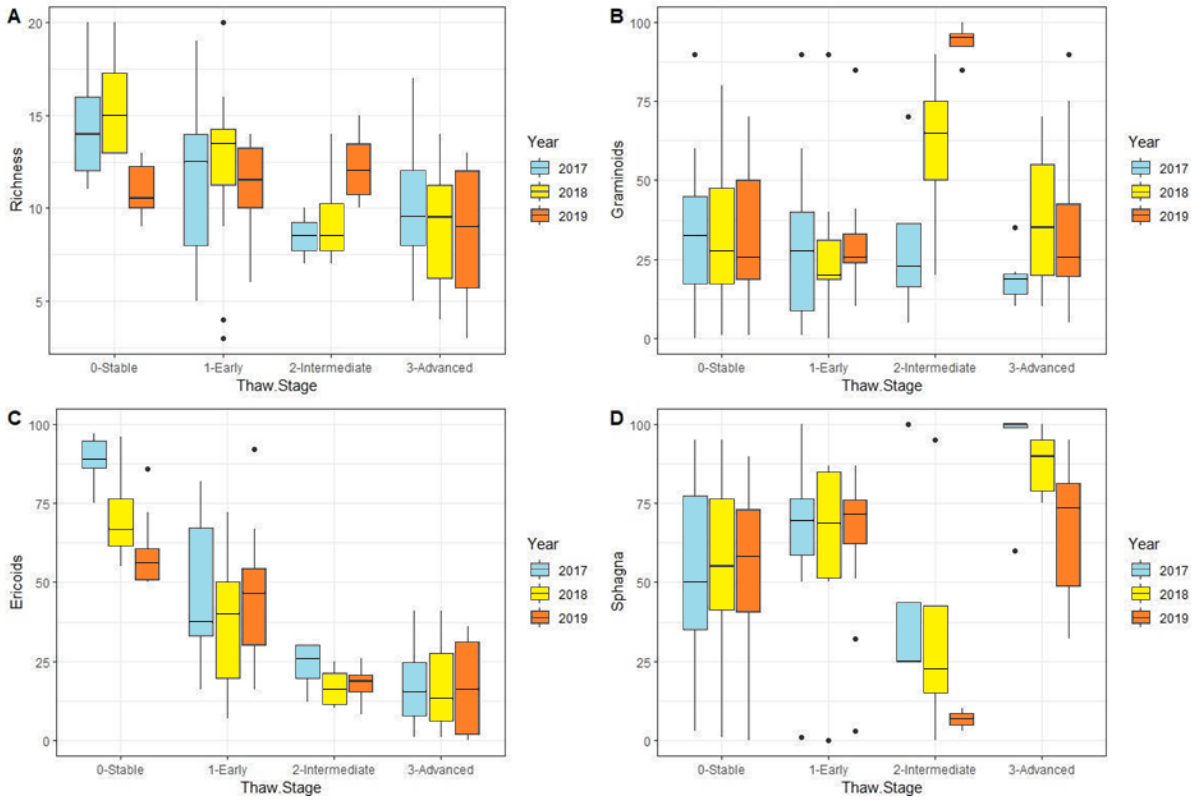

Figure 5. Plant species richness (A), Graminoid abundance (B), Ericoid abundance (C), and *Sphagnum* abundance (D) across the four stages of thaw (defined by variation in active layer thickness) across three sampling years.

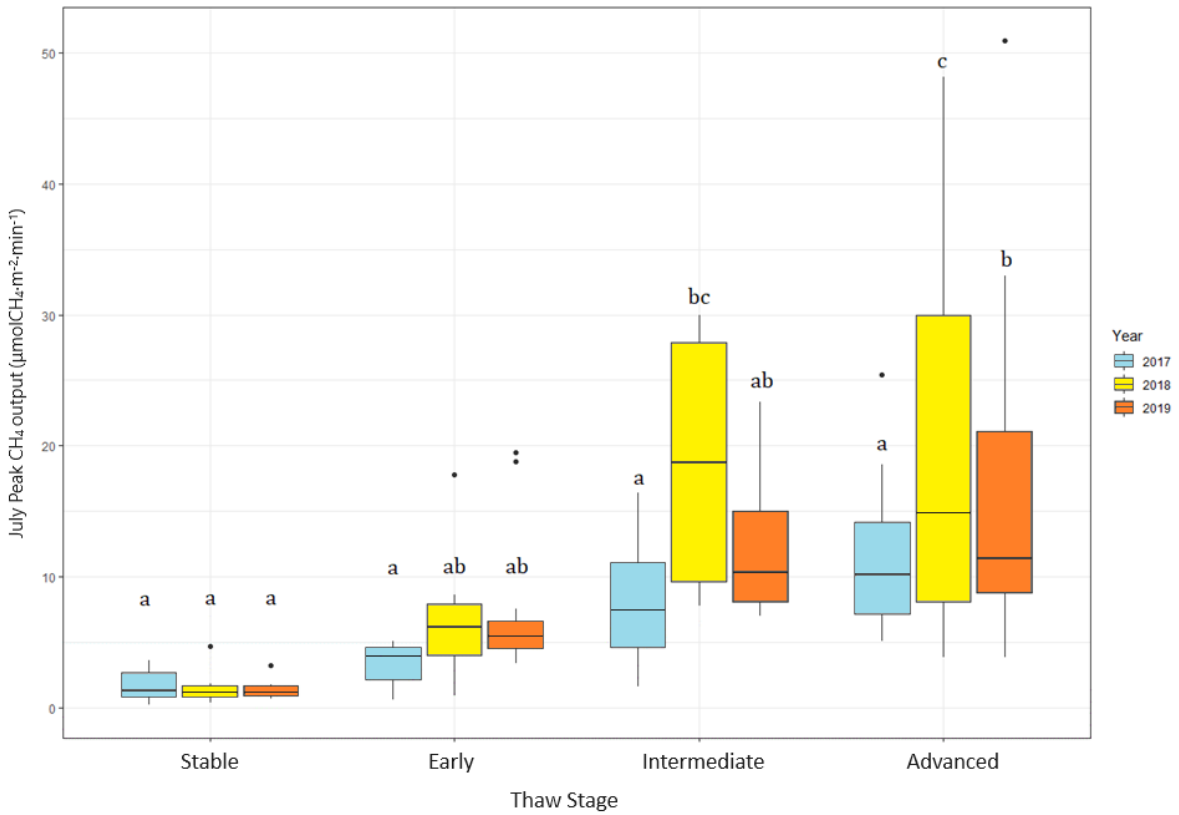

Figure 6. July methane flux at peak plant productivity over three years across the four thaw stages. Same letter superscripts denote nonsignificant differences between groups based on a post-hoc Tukey's HSD test.

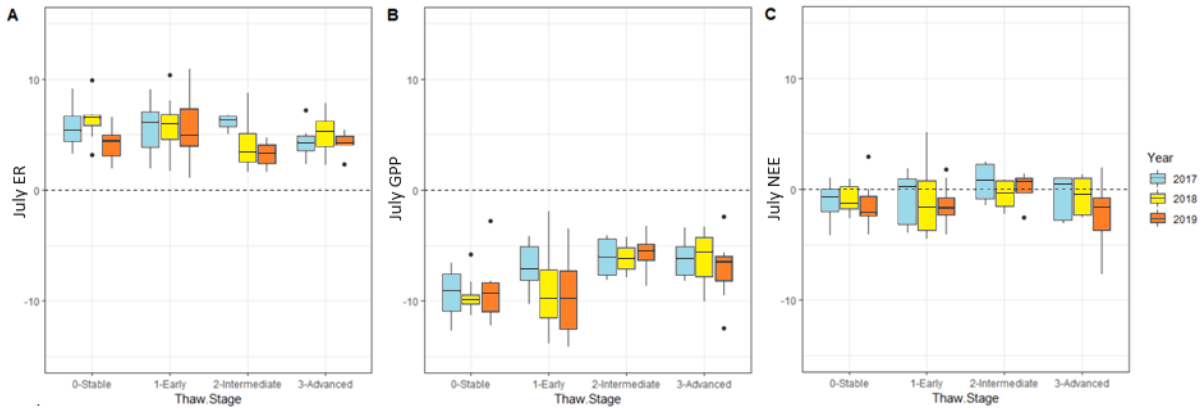

Figure 7. Ecosystem respiration (A), gross primary productivity (B), and net ecosystem exchange (C) in µmolC·m^{-2}·s^{-1}at summer peak productivity over three years across four thaw stages. Positive values indicate a net carbon source to the atmosphere while negative values indicate a net carbon sink.